Available online at www.sciencedirect.com
ScienceDirect
Journal of Power Sources 160 (2006) 765–772
JOURNAL OF POWER SOURCES
www.elsevier.com/locate/jpowsour

Heat generation in double layer capacitors

Julia Schiffer*, Dirk Linzen, Dirk Uwe Sauer

Electrochemical Energy Conversion and Storage Systems Group, Institute for Power Electronics and Electrical Drives (ISEA), RWTH Aachen University, Jaegerstrasse 17–19, D-52066 Aachen, Germany

Received 10 October 2005; received in revised form 15 December 2005; accepted 21 December 2005
Available online 7 February 2006

Abstract

Thermal management is a key issue concerning lifetime and performance of double layer capacitors and battery technologies. Double layer capacitor modules for hybrid vehicles are subject to heavy duty cycling conditions and therefore significant heat generation occurs. High temperature causes accelerated aging of the double layer capacitors and hence reduced lifetime. To investigate the thermal behavior of double layer capacitors, thermal measurements during charge/discharge cycles were performed. These measurements show that heat generation in double layer capacitors is the superposition of an irreversible Joule heat generation and a reversible heat generation caused by a change in entropy. A mathematical representation of both parts is provided.

Keywords: Double layer capacitor; Heat generation; Thermal behavior; Reversible heat effect

1. Introduction

Double layer capacitors, also known as supercapacitors or ultracapacitors, are energy storage devices which offer high power density, extremely high cycling capability and mechanical robustness. In contrast to batteries, double layer capacitors do not undergo a chemical reaction in order to store energy. The working principle is based on an electrostatic effect, which is purely physical and therefore highly reversible. Recent technology improvements enabled double layer capacitors to be an interesting option for short-term high power applications, such as in industry, automotive and traction drives, medical and telecommunication equipment [1–3].

They consist of two activated carbon electrodes, which are immersed into an ionic electrolyte. The two electrodes are separated by a membrane, which allows the mobility of the charged ions but prevents electric contact. When the electrodes are charged, the ions of the electrolyte move towards the electrode surface of the opposite charge. In the charged state, the anions and cations are located in the electrolyte next to the electrodes such that they balance the excess charge on the electrical conduction side (solid state electrode material) of the phase boundary. Thus, there are two layers of excess charge of opposite polarity across the phase boundary. This layer is called an electrochemical double layer or Helmholtz layer and was discovered in 1879 by Helmholtz. Upon discharge, the ions move back towards the bulk of the electrolyte [3].

Additionally to the double layer capacitance associated to the process of storing charge in the electrostatic double layer, a second kind of capacitance, the so-called pseudocapacitance, can be observed in double layer capacitors. Two types of pseudocapacitances can arise in electrochemical processes: adsorption of hydrogen atoms and redox processes [4]. According to Ref. [3], the first type occurs mainly in supercapacitors with carbon electrodes and aqueous electrolyte. Supercapacitors with carbon electrodes and organic electrolyte show only very little pseudocapacitative behavior (adsorption type) [3], which results in a slightly higher capacitance that cannot be separated from the double layer capacitance in capacitance measurements. Redox processes occur in supercapacitors with metal oxide (e.g. RuO_2 or IrO_2) or polymer electrodes [2–4]. The experimental and theoretical investigations for this paper have been done for double layer capacitors with carbon electrodes and organic electrolyte. These materials are the basis for the commercial products on the market today for devices with several hundred to several thousand farads.

* Corresponding author. Tel.: +49 241 8096935; fax: +49 241 8092203.
E-mail addresses: sf@isea.rwth-aachen.de (J. Schiffer), li@isea.rwth-aachen.de (D. Linzen), sr@isea.rwth-aachen.de (D.U. Sauer).

0378-7753/$ – see front matter © 2006 Elsevier B.V. All rights reserved.
doi:10.1016/j.jpowsour.2005.12.070

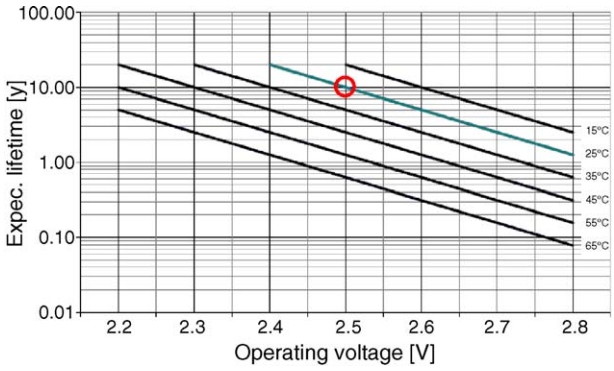

Fig. 1. Life expectancy of double layer capacitors vs. operating voltage and cell temperature [5]. Lifetime at nominal conditions (25 °C, 2.5 V/cell) is 10 years.

Double layer capacitors are capable of undergoing several hundred thousands deep discharge and charge cycles because of the high reversibility of the charging and discharging process. In contrast to batteries, cycling stress has a reduced influence on aging of the capacitor.

Parasitic electrochemical reactions of the electrolyte, such as oxidation, are accelerated at higher temperatures, according to Arrhenius law, and similarly at increased voltages. As a consequence of this continuous process, the capacitance decreases, while internal resistance and self-discharge rate rise. In Fig. 1 the typical influence of cell voltage and temperature on the degradation of double layer capacitors is given [5]: lifetime is halved for each 100 mV above nominal voltage (here 2.5 V) and for each 10 K above 25 °C.

Due to the strong dependency on temperature, it is necessary to know the thermal behavior of double layer capacitors. A thermal simulation model is a valuable tool for the design of future cells and modules as well as for cooling strategies. It is therefore of great importance to find a mathematical representation of the heat generation mechanisms. Based on impedance measurements and charge/discharge tests, the heat generation mechanisms in double layer capacitors were identified and a mathematical representation was found and verified.

1.1. Impedance based modeling approach

The electric equivalent circuit (Fig. 2) of a double layer capacitor cell, which can be derived from impedance measurements, consists of an inductance, a series resistance and the pore impedance $\underline{Z}_p$ [1,6–8].

The inductance L describes the inductive behavior of the cell including the terminals and R_s is the ohmic series resistance of the double layer capacitor, which represents the ohmic losses in contacts, electrodes and bulk electrolyte [3].

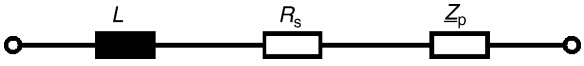

Fig. 2. Equivalent electric circuit of a double layer capacitor [6].

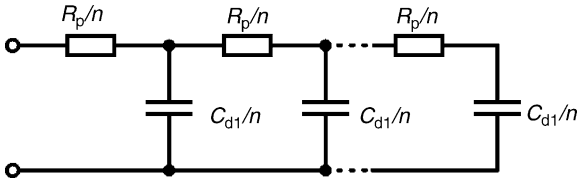

Fig. 3. Equivalent circuit of the impedance of a porous electrode [7].

Table 1
Impedance values obtained from fitting impedance data to the model described in Section 1.1 for Nesscap 5000 F and Nesscap 600 F at room temperature

Voltage (V)	R_s (mΩ)	C_{dl} (F)	R_p (mΩ)	L (nH)
Nesscap 5000 F				
0.5	0.236	4850	0.0673	22
1.5	0.238	4900	0.0761	22
2.5	0.243	5000	0.0984	22
Nesscap 600 F				
0.675	0.545	646.8	0.405	16.6
1.35	0.529	640.9	0.459	16.6
2.025	0.56	648.3	0.45	16.6
2.7	0.586	655.8	0.867	16.6

The complex impedance $\underline{Z}_p$ with

$$Z_p = \sqrt{\frac{R_p}{j\omega C_{dl}}}\,\coth\left(\sqrt{j\omega R_p C_{dl}}\right) \tag{1}$$

is the impedance of the porous electrodes [9,10]. C_{dl} is the capacitance of the double layer and R_p is the resistance of the electrolyte in the pores. $\underline{Z}_p$ can be approximated by an RC ladder network (Fig. 3) with an infinite number of elements according to Refs. [9–11].

1.2. Joule heat generation

The resulting Joule heat generation dQ_{Joule}/dt is the power loss in the ohmic resistances:

$$\frac{dQ_{Joule}(t)}{dt} = P_{Loss}(t) = i(t)^2 R_s + \sum_{k=1}^{n} i_k(t)^2 \frac{R_p}{n}, \tag{2}$$

where $i(t)$ is the applied current, R_s the series resistance, R_p/n the resistance of one element of the equivalent ladder circuit (Fig. 3) and i_k is the current through the resistance of the kth ladder element.

Using an impedance based model, the heat generation as a function of the ladder network can be calculated. Impedance values obtained from measurements at room temperature (Table 1) were applied for simulation. Measurements have shown that the impedance values depend very little on the applied current,[1] but show greater changes with voltage. Hence, only the voltage dependency is considered. Fig. 4 shows the simulated heat

[1] The range of the applied DC currents was 0 to ±40 A for the 5000 F supercap. With the surface of the porous electrodes being about 25,000–50,000 m^2 for this supercap (see Section 3.2), this corresponds to a maximum current density of 0.8–1.6 mA m^{-2}. Related to the capacitance this is 0.2 A F^{-1}.

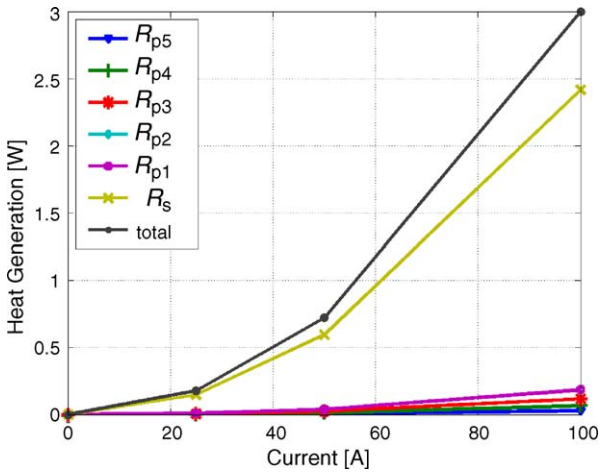

Fig. 4. Example for the calculated heat generation I^2R in the resistances of the equivalent circuit for different constant charging currents for a ladder network with five branches. Impedance values are for a Nesscap 5000 F supercapacitor. All R_p values are equal.

generation for a ladder network with five branches for a Nesscap 5000 F during charging with a constant current. Ohmic losses in the series resistance R_s represent in this case about 80% of the total heat generation. The percentage of the different resistances on the overall heat generation is nearly independent from the applied current. Hence, if the resistance of the pore impedance was neglected for heat calculation, the calculated heat would be about 20% too low. For a Nesscap 600 F, the simulated losses in the series resistance represent only 60% of the total heat generation (Fig. 5).

Differences in the distribution of the heat generation originate from the different R_s to R_p ratio for the two devices. For the Nesscap 5000 F, R_s is about three times higher than R_p, while the two resistances have about the same value for the Nesscap 600 F. The electrode structure can be assumed to be similar for the two devices as they belong to the same product series from Nesscap. Hence, the difference seems to result from the different cell size

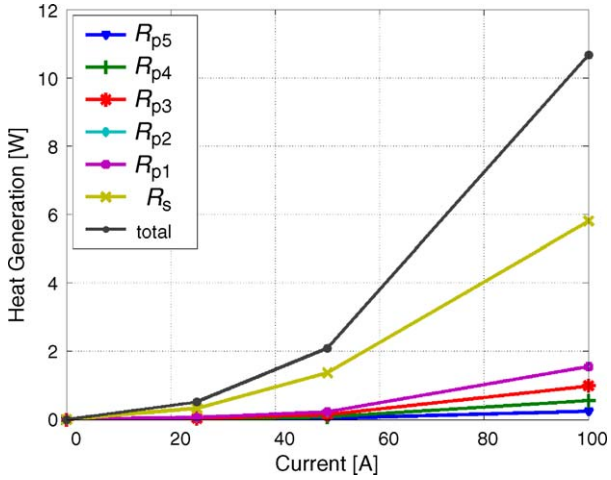

Fig. 5. Example for the calculated heat generation I^2R in the resistances of the equivalent circuit for different constant charging currents for a ladder network with five branches. Impedance values are for a Nesscap 600 F supercapacitor. All R_p values are equal.

(electrode resistance) and relatively high contact resistance in the 5000 F supercap.

2. Measurements

The measurements which will be reported in this section were done using a double layer capacitor ESHSP-5000C0-002R7 by Nesscap with 5000 F (Fig. 6).

In the following sections, the results of temperature measurements during charge/discharge cycles with various currents are presented and analyzed.

2.1. Experimental setup

For precise measurements, it is useful that the influence of convection and radiation can be neglected. Measurements with the double layer capacitor inside a box of polystyrene can be considered as quasi-adiabatic (nearly no heat exchange with the surrounding). The time constant of box and supercap together is about 3 h. Temperature sensors AD590 from Analog Devices have been used that deliver a temperature dependent current ($1\ \mu A\ K^{-1}$) if a voltage of 4–30 V is supplied. The sensors are fixed to the surface of the supercap with a rubber band and with a piece of polystyrene to assure a constant pressure. The temperature is measured at two points on the supercap surface to get additional information about the heat distribution.

Fig. 6. Double layer capacitor 5000 F Nesscap.

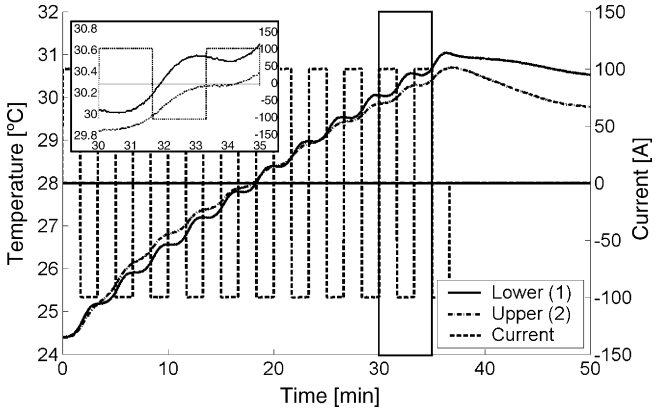

Fig. 7. Test with Nesscap 5000 F, 100 A, 0.5–2.5 V, the duration of each phase is 100 s.

The test profiles consist of alternating charge and discharge cycles of the same duration in three different voltage ranges (0.5–1.5, 1.5–2.5 and 0.5–2.5 V) to find out about the influence of voltage. To make the tests comparable regarding the total duration, the tests with only 1 V range consist of 22 charge and discharge cycles and the test with 2 V range consists of 11 charge and discharge cycles. The duration of each phase is set to

$$\Delta t = \frac{C\,\Delta U}{I}. \tag{3}$$

Fig. 7 illustrates as an example the current and temperature curves for a test with ±100 A (current density in the range of 2–4 mA m^{-2} or 2 A F^{-1}) in the range 0.5–2.5 V. The duration of each charge and discharge step is 100 s. Both temperature curves (1 and 2) are relatively close to each other, so both temperature values can be assumed to be a good representation of the supercap temperature. Because of the cables for measurement and power supply, the polystyrene box can never be completely closed and the upper part of the double layer capacitor will always be more influenced by the environment than the lower part. Thus, only the temperature at point 1 is regarded for further analysis.

The inset of Fig. 7 shows a zoom of the three curves near the end of the test. Temperature begins to rise towards the end of a charging step and begins to fall towards the end of a discharging step. Both the rise and the drop start clearly before the next step starts. Hence, it can be concluded that the temperature rise is caused by charging and that the temperature drop is caused by discharging and not vice versa. The delay of the temperature curves can be explained by the fact that heat is generated inside the supercap. Since the temperature sensors are mounted on the supercap surface, it takes some time until the heat can be detected.

2.2. Impact of constant current charge/discharge

Fig. 8 depicts the comparison of the temperature at point 1 for two tests that consist of eleven charge and discharge steps with ±100 A between 0.5 and 2.5 V, once with discharge first and once with charge first. The duration of each step is 100 s. To make the measurements comparable, the initial temperature is

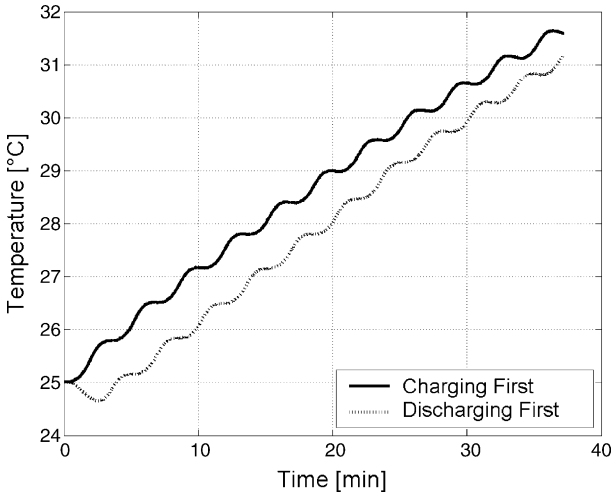

Fig. 8. Comparison of tests with discharge first or charge first, Nesscap 5000 F, 100 A, 0.5–2.5 V, duration of each step is 100 s.

set to 25 °C. Both curves show a temperature rise of about 6.5 K. Additionally to the almost linear rise that can be expected from Joule heat, a ripple can be seen in both curves. This ripple is also depicted in Fig. 9, calculated from the measured temperature minus a linear rise of about 3 mK s^{-1}. If the test starts with a discharge step, the temperature falls in the beginning. Hence, it can be concluded that a double layer capacitor is cooled during a discharge step.

Similar tests were taken at the two other voltage ranges, 0.5–1.5 and 1.5–2.5 V. Again, the current is ±100 A, but the duration of each step is 50 s because of the smaller voltage range. The results are similar, but the amplitude of the ripple is different for the three voltage ranges. The highest amplitude can be measured at 0.5–2.5 V; the amplitudes at the two other ranges are smaller and close to each other.

2.3. Impact of the current rate

Fig. 10 compares the temperature curves of tests with different currents, 100, 50 and 25 A, all at 1.5–2.5 V. Looking at

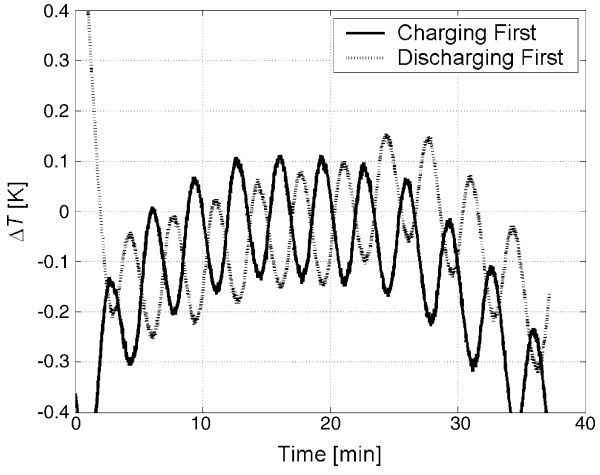

Fig. 9. Ripple of tests with discharge first or charge first, Nesscap 5000 F, 100 A, 0.5–2.5 V, duration of each step is 100 s.

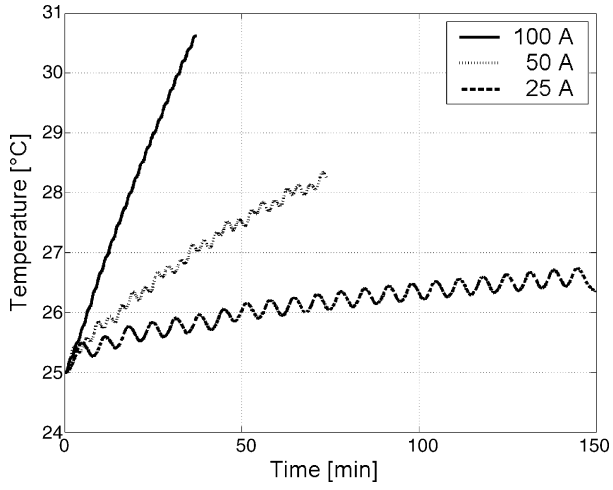

Fig. 10. Current dependency for 100, 50 and 25 A, Nesscap 5000 F, 1.5–2.5 V. The duration of each step is 50 s for 100 A, 100 s for 50 A and 200 s for 25 A, first step is charging.

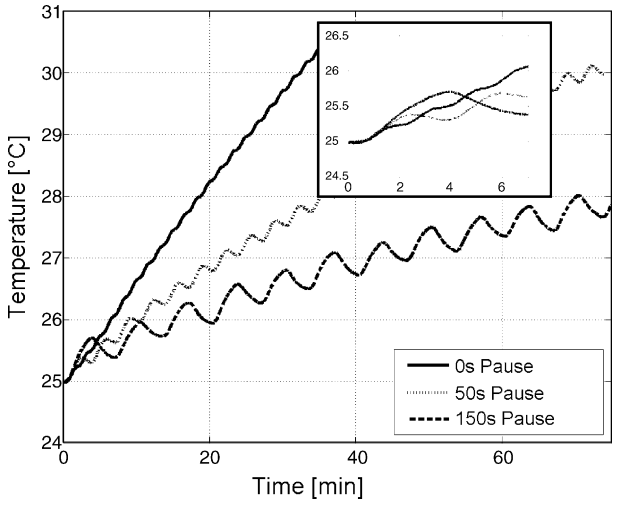

Fig. 11. Influence of the duration of the steps, Nesscap 5000 F, 100 A, 1.5–2.5 V. The duration of each step including the pause is 50 s for the test without pause, 100 s for the test with 50 s pause and 200 s for the test with 150 s pause, first step is charging. *Inset*: Zoom of the beginning of the tests.

the gradient of the total temperature rise, it can be found that the total temperature rise is proportional to the squared current which corresponds to the Joule heat (Eq. (2)).

Using the impedance based model and the parameters for the model shown in Section 1.1, the generated heat ΔQ can be calculated. Together with the heat capacitance C_{Heat} of the supercap the theoretical temperature rise ΔT can be determined.

$$\Delta T = \frac{\Delta Q}{C_{\text{Heat}}}. \tag{4}$$

The heat capacitance of the Nesscap 5000 F was measured during cooling from 50 °C to room temperature. The measured value of about 1118 kJ K^{-1} fits well with calculations taking into account the materials and the inner geometry.

Table 2 lists the comparison of measured and calculated temperature rise. The values are very close. Differences between the measured and calculated values may result from temperature dependencies of the impedance values which are not considered in the calculation and from possible leaks in the polystyrene box. Noticeably, the measured value for 100 A is below the calculated value, while the measured values for 50 and 25 A are above the calculated value. A possible reason for this is the current distribution in the supercap. At higher current rates, also the frequency of the square pulse is higher and most of the current flows through the upper half of the supercap, while the current distribution is more homogeneous at lower frequencies (lower currents). The measurement was done in the lower part of the supercap, but the calculation is the average supercap temperature. Hence, the measured temperature at 100 A is probably lower than the average temperature. However, the comparison indicates that the temperature rise corresponds to the Joule heat.

Table 2
Comparison of measured and calculated temperature rise for different current values, Nesscap 5000 F, 1.5–2.5 V. The time span is the duration of the complete test

Current (A)	Measured ΔT (K)	Calculated ΔT (K)	Δt (s)
100	5.5	6.06	2200
50	3.2	3.01	4400
25	1.6	1.51	8800

2.4. Impact of the cycle duration

Heat generation occurs inside the supercap. Since the measurement only can be done on the surface, a certain delay occurs between the heat generation and the measurement. Additionally, the effects of heating during charging and cooling during discharging overlap and influence each other. To determine the ripple as precisely as possible, pauses were added after each step. Fig. 11 shows the comparison of tests at 1.5–2.5 V and 100 A with different duration of the pause after each charging and discharging step. The first test is without pause, the second with 50 s pause after each step and the third with 150 s pause. It can be seen, especially in the inset, that the amplitude of the ripple becomes higher with increasing pause duration and that the superposed ripple of the test with 150 s pause no longer looks like a sine wave, but has an exponential shape during each pause.

2.5. Summary and conclusion of the measurements

All temperature curves presented above consist of an almost linear part with a superposed ripple, which can be referred to as a reversible heat effect. The linear part proved to be caused by Joule heat generation. Further investigations of the wave line have shown that the double layer capacitor is cooled during discharge and additionally heated during charge. The amplitude of the ripple increases with the duration of each step. If a pause is added after each charge and discharge step, the shape of the ripple becomes more and more exponential, so that more and more of the total ripple becomes visible at the surface. Because of the thermal resistances and capacitances it takes some time for the total temperature change to reach the surface.

Table 3
Temperature change during the measurements with the Nesscap 5000 F

Test	Voltage range (V)	First step	Current (A)	Pause (s)	Duration incl. pause (s)	ΔT (K)
1, 4	0.5–1.5	Charge, discharge	100	0	50	0.05
2, 5	1.5–2.5	Charge, discharge	100	0	50	0.06
3, 6	0.5–2.5	Charge, discharge	100	0	100	0.22
7	1.5–2.5	Charge	50	0	100	0.15
8	1.5–2.5	Charge	25	0	200	0.3
9	1.5–2.5	Charge	100	50	100	0.2
10	0.5–1.5	Charge	100	150	200	0.45
11	1.5–2.5	Charge	100	150	200	0.45
12	0.5–2.5	Charge	100	150	250	0.9

Similar tests with a B49400 EPCOS 3600 F (cylindrical) and a ESHSP-0600C0-002R7 NESSCAP 600 F (prismatic) have shown a similar behavior.

3. Reversible heat effect

Table 3 lists all measurements with the Nesscap 5000 F and the temperature ripple, further on called the reversible heat. Tests 3 and 6 are compared in Fig. 8. Fig. 10 shows a comparison of tests 2, 7 and 8 and Fig. 11 shows the comparison of tests 2, 9 and 10. Tests 1, 4, 5, 11 and 12 are not illustrated. They are added here for completeness.

The last three tests all include a pause of 150 s after each charge and discharge step. This pause separates the effect of charge and discharge and allows therefore to find out the "real" temperature difference. Longer pauses have the drawback that the thermal contact to the environment influences the measurements increasingly.

Extracting the internal temperature difference between a charging and a discharging step is difficult, because only retarded temperature values at the device surface are available. For measurements 1–9 in Table 3 only the differences between maximum and minimum of the temperature ripple are analyzed. However, this is not giving a clear indication for the temperature inside the device. Thus, for the evaluation of tests 10–12, which include rest periods of 150 s after each charge or discharge cycle, a more sophisticated approach has been chosen. The temperature curves for each charge or discharge cycle have been fitted by an exponential curve (see Fig. 12). The fitted curves allow an extrapolation to the equilibrium temperature and from this extrapolation, the full temperature difference was taken. For the example shown in figure Fig. 12 (test 12) the temperature difference is 0.9 K for a cycle from 0.5 to 2.5 V. If only 50% of the charge is taken from the supercap (tests 10 and 11), the temperature difference amounts to 0.45 K.

Three possible causes for a reversible heat generation have been further looked at: a chemical reaction, the Peltier effect and a change in entropy. The first two causes could be sorted out because the only known reversible chemical reaction in double layer capacitors, the redox pseudocapacitance process, can be neglected in double layer capacitors with carbon electrodes and organic electrolyte as they are investigated here (see discussion in Section 1). The Peltier effect for a contact of aluminum and coal would result in a temperature change of some μK that is proportional to the applied current, but the results from the tests listed in Table 3 show a change of between 0.05 and 0.9 K without any proportionality to the current.

This leaves the entropy as explanation for the reversible heat generation. Since the ions in the electrolyte of a double layer capacitor are arranged in the electric field during charging and are spreading themselves again during discharging and entropy can be interpreted as a measure for disorder, this is a suitable explanation.

3.1. Mathematical representation

For the derivation of the equations one has to divide the double layer capacitor system into two subsystems: the system of the ions and the system of the remaining parts of the double layer capacitor.

According to Ref. [12] the change in entropy of a reversible process from state 1 to state 2 is

$$\Delta S = \int_1^2 \frac{\mathrm{d}Q_{\mathrm{rev}}}{T}, \tag{5}$$

where Q_{rev} is the added or removed heat of the reversible process and T is the temperature. Since the reversible process in the double layer capacitor only concerns the ions, Eq. (5) corresponds to the system of the ions. Seen from the view of the remaining

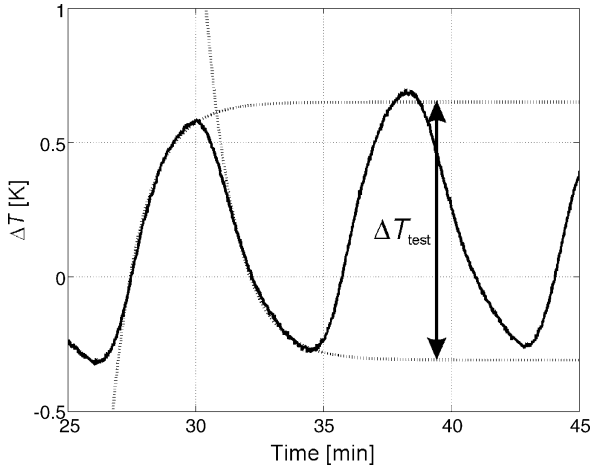

Fig. 12. Zoom of the temperature ripple for test 12, Nesscap 5000 F, 100 A, 0.5–2.5 V with a pause of 150 s and approximative exponential curves for charging and discharging.

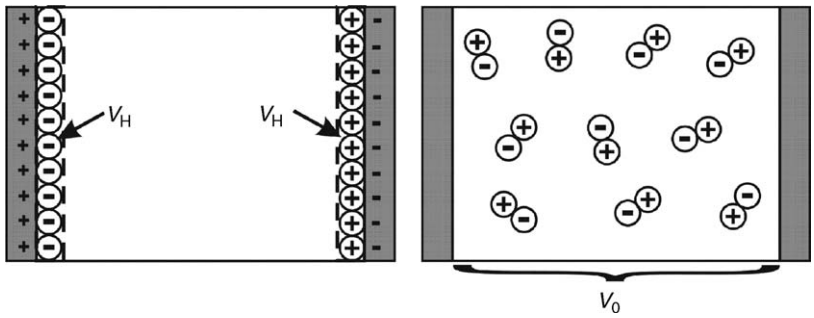

Fig. 13. Ion distribution in the electrolyte for charged (left) and discharged (right) condition.

double layer capacitor, which is what one can observe with the measurements, the sign must be reversed because the entropy that is added to the ions' system is taken from the remaining supercap system and vice versa:

$$\Delta S = -\int_1^2 \frac{\mathrm{d}Q_{\mathrm{rev,meas}}}{T}. \tag{6}$$

With $\mathrm{d}Q_{\mathrm{rev,meas}} = C_{\mathrm{Heat}}\,\mathrm{d}T$, where C_{Heat} is the heat capacitance of the double layer capacitor, the integral can be calculated:

$$\Delta S = -\int_1^2 \frac{C_{\mathrm{Heat}}\,\mathrm{d}T}{T} = -C_{\mathrm{Heat}} \ln\left(\frac{T_2}{T_1}\right). \tag{7}$$

In general, the entropy of a system is determined by the probability p to realize a defined state of the system and the Boltzmann constant $k = 1.380658 \times 10^{-23}\,\mathrm{J\,K^{-1}}$ [12]

$$S = k \ln p. \tag{8}$$

As an example, the probability of N particles to be located in a subvolume V_1 of the total volume V is given as [12]

$$p = \left(\frac{V_1}{V}\right)^N. \tag{9}$$

To calculate the entropy change of the system, the increasing and decreasing number of ions in the volume of the double layer V_{H} is regarded. Fig. 13 shows a view of the ion distribution in the electrolyte between positive and negative electrode under the simplified assumption of a double layer (Helmholtz layer) with constant capacitance and constant dimensions (plate condenser model). The left picture represents the (ideally) charged capacitor, where all ions have moved to the surface of the electrodes to compensate the positive and negative charges on the electrodes. Now, all ions of one kind are in the same double layer. This is the state of maximum order and therefore minimum entropy. In the (ideally) discharged condition, no charges are left on the electrodes and the ions fill the whole electrolyte volume similar to an ideal gas. This represents the state of maximum disorder and therefore maximum entropy.

The electrolyte of most double layer capacitors consists of the salt tetraethyl ammonium borofluoride (TEABF) dissolved in the solvent acetonitrile. The chemical formula of TEABF is $(C_2H_5)_4NBF_4$, the solved salt forms $(C_2H_5)_4N^+$ and BF_4^- ions which are monovalent. A double layer capacitor with the total capacitance C consists of a series connection of two double layers with the capacitance $2C$. To build up a voltage U ($U/2$ for each of the double layers), N ions of each kind are arranged in the electrolyte to counterbalance the charge $N \times e$ on each of the electrodes. Hence, N can be calculated as:

$$N = \frac{2CU/2}{e} = \frac{CU}{e}. \tag{10}$$

The entropy of one kind of ions is related to the probability that N ions are located within the volume V_{H} of the Helmholtz layer:

$$S_{\mathrm{one\,kind}} = k \ln\left(\frac{V_{\mathrm{H}}}{V_0}\right)^N. \tag{11}$$

V_0 is the total electrolyte volume.

For a more simplified mathematical representation, the volumes of both Helmholtz layers are assumed to be equal, although the ions are of different sizes. In literature, the thickness of the Helmholtz layer, which is in the range of the size of the ions, is typically not distinguished for the two electrodes.

The entropy of both kinds of ions together is

$$S = 2S_{\mathrm{one\,kind}} = 2k \ln\left(\frac{V_{\mathrm{H}}}{V_0}\right)^N. \tag{12}$$

With Eq. (10), Eq. (12) becomes

$$S = 2k\frac{CU}{e} \ln\left(\frac{V_{\mathrm{H}}}{V_0}\right). \tag{13}$$

With the assumption that the dimensions of the Helmholtz layer are constant, the time derivative of the entropy is

$$\frac{\mathrm{d}S}{\mathrm{d}t} = \frac{2Ck}{e} \ln\left(\frac{V_{\mathrm{H}}}{V_0}\right)\frac{\mathrm{d}U}{\mathrm{d}t}. \tag{14}$$

The reversible heat can then be calculated with:

$$\frac{\mathrm{d}Q_{\mathrm{rev,meas}}}{\mathrm{d}t} = -T\frac{\mathrm{d}S}{\mathrm{d}t} = -2T\frac{Ck}{e} \ln\left(\frac{V_{\mathrm{H}}}{V_0}\right)\frac{\mathrm{d}U}{\mathrm{d}t}. \tag{15}$$

With $\mathrm{d}U/\mathrm{d}t = i(t)/C$ this becomes

$$\frac{\mathrm{d}Q_{\mathrm{rev,meas}}}{\mathrm{d}t} = -2\frac{Tk}{e} \ln\left(\frac{V_{\mathrm{H}}}{V_0}\right) i(t). \tag{16}$$

Table 4
Calculated values a for the Nesscap 5000 F

Test	ΔU (V)	ΔT (K)	a	$\Delta a/a_{\text{average}}$
10	1	0.45	1.958	2.5E−04
11	1	0.45	1.958	2.5E−04
12	2	0.9	1.956	−5.0E−04
Average			1.957	

3.2. Verification

The factor $-\ln(V_H/V_0)$ will be called a in the following. a can be determined from the measurements with Eqs. (7) and (15):

$$\Delta S = \frac{2Ck}{e} \ln\left(\frac{V_H}{V_0}\right) \Delta U = -C_{\text{Heat}} \ln\left(\frac{T_2}{T_1}\right), \tag{17}$$

$$\Rightarrow -\ln\left(\frac{V_H}{V_0}\right) = a = \frac{C_{\text{Heat}} e}{2Ck\,\Delta U} \ln\left(\frac{T_2}{T_1}\right). \tag{18}$$

Table 4 lists the resulting values for a for the Nesscap 5000 F. They are calculated from the tests 10–12 because they have a relatively long pause between charging and discharging, so that it can be assumed that the superposition of heating from charging and cooling from discharging is sufficiently low. The parameters used for the calculation are: $C_{\text{Heat}} = 1118\,\text{J K}^{-1}$, $C = 5000\,\text{F}$, $T_1 = 298\,\text{K}$ and $T_2 = T_1 + \Delta T$.

The volumes V_H and V_0 can be estimated with the following assumptions. According to Ref. [13] the capacitance related to the geometric electrode surface is $1\,\text{F cm}^{-2}$ and related to the porous electrode surface 10–20 $\mu\text{F cm}^{-2}$. With a capacitance of 5000 F, the geometric surface is $A_0 = 0.5\,\text{m}^2$ and the porous surface A_H is 25,000–50,000 m^2. Under the assumption that the electrodes are a stack of wound layers and that the case is about 5 mm thick, the average width w of the windings is about 5 cm. Assuming that the height of the electrodes is about 12.5 cm, the geometric length l of the unwound electrodes results to be about 4 m. The total number of layers n can be approximated by

$$n = \frac{l}{w} = 80. \tag{19}$$

The thickness of one electrode layer including separator and electrolyte is approximately

$$d_{\text{layer}} = \frac{6\,\text{cm}}{n} = 750\,\mu\text{m}. \tag{20}$$

According to Ref. [13], the thickness of the electrodes (aluminum plus carbon) is about 250 μm, which results in a thickness d_0 of about 500 μm for the separator including electrolyte. The Helmholtz layer has a thickness d_H of about 1 nm [13]. The resulting volumes are $V_0 = 250\,\text{cm}^2$ and $V_H = 25\text{–}50\,\text{cm}^3$. With these values, a results to a value between 1.609 and 2.303, which fits very well with the calculated value $a = 1.957$.

4. Summary and conclusions

Thermal measurements were performed on a double layer capacitor, which have shown that heat generation consists of an irreversible Joule heat and a reversible heat. Joule heat can be derived from the electric equivalent circuit of the double layer capacitor. Changes in entropy were found to be the cause for the reversible heat effect: ions in the electrolyte are ordered during charging and they mix themselves again during discharging. Since entropy is a measure of disorder, the ion movement causes an entropy change between charged and discharged condition. A mathematical representation of the resulting temperature change is provided and deduced. Calculations of the Helmholtz layer volume using literature values for the electrode surface affirm the deduced equation.

Acknowledgements

The authors would like to thank Oliver Bohlen and Dr. Abderrezak Hammouche from ISEA as well as Dr. Eckhard Karden and Erik Surewaard from Ford Research Center Aachen for many valuable discussions.

References

[1] B.E. Conway, Electrochemical Supercapacitors: Scientific Fundamentals and Technological Applications, New York, 1999, ISBN 0-306-45736-9.
[2] A. Burke, Ultracapacitors: why, how and where is the technology, J. Power Sources 91 (2000) 37–50.
[3] R. Kötz, M. Carlen, Principles and applications of electrochemical capacitors, Electrochim. Acta 45 (2000) 2483–2498.
[4] B.E. Conway, V. Birss, J. Wojtowicz, The role and utilization of pseudocapacitance for energy storage by supercapacitors, J. Power Sources 66 (1997) 1–14.
[5] EPCOS: UltraCapTM Double Layer Capacitors, A New Energy Storage Device for Peak Power Applications, Product Profile, 2002.
[6] S. Buller, E. Karden, D. Kok, R.W. De Doncker, Modeling the dynamic behavior of supercapacitors using impedance spectroscopy, IEEE Trans. Ind. Appl. 38 (2002) 1622–1626.
[7] S. Buller, Impedance-based simulation models for energy storage devices in advanced automotive applications, Ph.D. Dissertation, RWTH Aachen, Aachen, Germany, 2003.
[8] E. Karden, Using low-frequency impedance spectroscopy for characterization, monitoring, and modeling of industrial batteries, Ph.D. Dissertation, RWTH Aachen, Aachen, Germany, 2001.
[9] R. De Levie, Electrochemical response of porous and rough electrodes, in: Advances in Electrochemistry and Electrochemical Engineering, vol. 6, Wiley-Interscience, 1967, pp. 329–397.
[10] J.R. Macdonald (Ed.), Impedance Spectroscopy, Emphasizing Solid Materials and Systems, John Wiley and Sons, 1987.
[11] MEISP—Multiple Electrochemical Impedance Spectra Parameterization, User Manual, Version 3.0, Kumho Petrochemical R&D Center.
[12] E. Hering, R. Martin, M. Stohrer, Thermodynamik, in: Physik für Ingenieure, vol. 6, Springer-Verlag, Berlin, Heidelberg, New York, 1997 (Auflage, Chapter 3).
[13] A. Schwake, D. Hahn, Electrochemical Capacitors as Energy Storage Devices in Automotive Applications, vol. 2, Aachen Electronics Symposium, 2004.